A. I. Sulyman, A. T. Nassar, M. K. Samimi, G. R. MacCartney, T. S. Rappaport, and A. Alsanie, "Radio propagation path loss models for 5G cellular networks in the 28 GHz and 38 GHz millimeter-wave bands," *Communications Magazine, IEEE*, vol. 52, no. 9, pp. 78-86, September 2014

Radio Propagation Path Loss Models for 5G Cellular Networks in the 28 GHz and 38 GHz Millimeter-Wave Bands

Ahmed Iyanda Sulyman, AlMuthanna T. Nassar, Mathew K. Samimi, George R. MacCartney Jr., Theodore S. Rappaport, and Abdulhameed Alsanie

ABSTRACT

This article presents empirically-based large-scale propagation path loss models for fifth-generation cellular network planning in the millimeter-wave spectrum, based on real-world measurements at 28 GHz and 38 GHz in New York City and Austin, Texas, respectively. We consider industry-standard path loss models used for today's microwave bands, and modify them to fit the propagation data measured in these millimeter-wave bands for cellular planning. Network simulations with the proposed models using a commercial planning tool show that roughly three times more base stations are required to accommodate 5G networks (cell radii up to 200 m) compared to existing 3G and 4G systems (cell radii of 500 m to 1 km) when performing path loss simulations based on arbitrary pointing angles of directional antennas. However, when directional antennas are pointed in the single best directions at the base station and mobile, coverage range is substantially improved with little increase in interference, thereby reducing the required number of 5G base stations. Capacity gains for random pointing angles are shown to be 20 times greater than today's fourth-generation Long Term Evolution networks, and can be further improved when using directional antennas pointed in the strongest transmit and receive directions with the help of beam combining techniques.

Ahmed Iyanda Sulyman and Abdulhameed Alsanie are with King Saud University.

AlMuthanna T. Nassar is with Mobily Telecom Company and King Saud University.

Mathew K. Samimi, George R. MacCartney Jr., and Theodore S. Rappaport are with NYU Polytechnic School of Engineering.

INTRODUCTION

Fifth-generation (5G) cellular systems are likely to operate in or near the millimeter-wave (mmWave) frequency bands of 30–300 GHz, where vast spectrum currently exists with light use. At these mmWave frequencies, the wavelength is so small that highly directional, steerable antennas may be used in novel ways. As recently shown, and in this article, propagation is a bit more lossy in the mmWave bands when compared to today's ultra-high-frequency (UHF) and low microwave regimes. However, these lossy mmWave channels can be made more reliable, and in some cases with smaller propagation losses, than today's cellular networks when highly directional steerable antennas and beam combining techniques are used at the base station and at mobile devices [1–4].

The mmWave spectrum is attractive for future wireless systems because of the massive amount of raw bandwidth available for cellular and backhaul services [1]. The IEEE 802.11ad (WiGig) standard now delivers 7 Gb/s data rates in the unlicensed 60 GHz band, and new unlicensed backhaul products in this band are now on the market. As the cellular industry looks to scale up into the mmWave spectrum, carriers are likely to use the 28 GHz, 38 GHz, and 73 GHz bands that will eventually become available for future wireless technologies [2].

To understand radio propagation in dense urban mmWave cellular networks, extensive measurements have been carried out to characterize these bands for future cellular and backhaul systems for both indoor and outdoor environments, as well as for peer-to-peer applications [2, 4, 5]. The works in [1, 5] present general introductions to mmWave mobile communication systems, and integrated antenna and circuit structures for 60 GHz mmWave wireless systems are relatively well understood today [6]. Works in [2, 4] also present path loss and wideband propagation measurements for mmWave frequencies using highly directional rotatable horn antennas, where mmWave transmissions were observed to be more lossy, with path loss proportional to the square of the increase in frequency, but exhibit rich multipath scattering when considering narrow angular resolution at the receiver. Works in [3, 7, 8] present theoretical studies on the coverage, spectral efficiency, and outage analysis of mmWave transmissions, respectively. Results in [7, 8] also suggest that when high gain (e.g., 25 dBi), highly directional steerable antennas are used at the base and mobile stations, mmWave transmissions have higher probability of coverage than their present-day microwave counterparts that use omnidirectional antennas. In this article, we employ recent propagation models using a commercial field-level network simula-

0163-6804/14/$25.00 © 2014 IEEE

tor to show that mmWave systems in fact have *better* radio frequency (RF) coverage than today's cellular systems, and we provide new path loss models for large-scale path loss estimation when planning cellular networks, just as is now done in the UHF/microwave bands. Popular path loss models used by wireless carriers for system deployment and coverage/capacity modeling include the Free Space (FS) model, the Okumura model, the Hata/COST231-Hata model [9], the Stanford University Interim (SUI) model [10], and the close-in free space reference distance d^n model [11]. Here, we modify these popular models for use in mmWave bands, with the understanding that future work may offer further improvement using ray-tracing and scattering models [2, 3]. Large-scale propagation prediction has been the fundamental technique used for cellular planning and design since the advent of the cellular industry, where carrier frequencies have only moved from 450 MHz (first generation cellular) to 2–3 GHz (today). New path loss prediction models for use in the mmWave bands in various localities around the world are still not well known, and early propagation measurements and models have only recently become available [2, 4, 8]. In this article, we propose modifications to the popular FS and SUI models, using extensive empirical measurements made over the past several years in New York City and Austin, Texas, to provide several path loss prediction models for the 28 and 38 GHz mmWave bands.

The rest of this article is organized as follows. We first present the path loss models for microwave and mmWave cellular systems; next, we present the RF coverage analysis for microwave and mmWave networks, and then present the conclusion of the article.

Outdoor Path Loss Prediction for Cellular Networks in the Microwave and MmWave Bands

Path Loss Models for UHF/Microwave Band

Path loss, which dictates the RF coverage distance (i.e., cell size) for cellular systems employing omnidirectional antennas, is generally inversely proportional to the square of the carrier frequency, as modeled by the Friis free space path loss formula [11]. In cellular planning, path loss must be estimated for a deployment environment, and cell coverage is determined based on the base station (BS) and mobile station (MS) antenna gains, effective isotropic radiated power (EIRP), RF bandwidth, and modulation and coding techniques. Omnidirectional large-scale path loss in urban environments may be estimated from the Hata model and the COST231 extension of the Hata model for carrier frequency (f_c) below 2 GHz [9, 11], and from the SUI model for f_c above 2 GHz [10]:

$$PL_{\text{SUI}}(d) = PL(d_0) + 10n\log_{10}\left(\frac{d}{d_0}\right) + X_{f_c} + X_{\text{RX}} + X_\sigma \quad (1)$$

where

$$PL(d_0) = 20\cdot\log_{10}\left(\frac{4\pi d_0}{\lambda}\right) \quad (1a)$$

$$n = a - b\cdot h_{TX} + \frac{c}{h_{TX}} \quad (1b)$$

$$X_{f_c} = 6\cdot\log_{10}\left(\frac{f_{\text{MHz}}}{2000}\right), f_c > 2\ \text{GHz} \quad (1c)$$

$$X_{RX} = -10.8\cdot\log_{10}\left(\frac{h_{RX}}{2}\right) \quad (1d)$$

and λ is the carrier wavelength in meters, $PL(d_0)$ in Eq. 1a denotes the free space path loss in dB at a close-in reference distance d_0; X_{fc}, and X_{RX} in Eq. 1d denote the correction factors for frequency and receiver heights, respectively, and X_σ in Eq. 1 is the typical lognormal random shadowing variable with 0 dB mean and standard deviation σ [dB] such that $8.2 < \sigma < 10.6$ dB [10]. f_{MHz} in Eq. 1c is the carrier frequency (f_c) in MHz; h_{TX} and h_{RX} denote the transmitter (TX) and receiver (RX) antenna heights in meters, respectively. The parameters a, b, and c in Eq. 1c are constants used to model the terrain types encountered in the service area. Here we consider the model suited for hilly and dense vegetation (denoted SUI terrain type A), with parameters given as $a = 4.6$, $b = 0.0075$, and $c = 12.6$ [10]. The path loss model in Eq. 1 is used to engineer cellular systems in many markets throughout the world, including Saudi Arabia.

Proposed Path Loss Models for MmWave Bands

Using recent field data, we now propose several empirical path loss models suitable for estimating steerable single beam mobile systems (using high gain, narrowbeam antennas at the TX and RX) for 5G mmWave cellular networks in the 28 GHz and 38 GHz bands. The 28 and 38 GHz measurements were performed using a broadband sliding correlator channel sounder, using identical binary phase shift keying (BPSK) modulated pseudo-noise (PN) maximal length sequences with chip lengths of 2047 and clocked at 400 megachips per second (Mcps) and 750 Mcps, respectively. The 28 GHz campaign employed both 10.9° and 28.8° half-power beamwidth (HPBW) antennas at the TX and RX, while the 38 GHz campaign employed a 7.8° HPBW antenna at the TX, and both a 7.8° and a 49.4° HPBW antenna at the RX [2, 4, 8]. The propagation measurement campaigns in [2, 4, 8] recorded power delay profiles (PDPs) for unique pointing angles using highly directional

5G cellular systems are likely to operate in or near the mm-wave frequency bands of 30–300 GHz, where vast spectrum currently exists with light use. At these mm-wave frequencies, the wavelength is so small that highly directional, steerable antennas may be used in novel ways.

Frequency: 28 GHz				
Environment	**NLOS**		**LOS**	
TX height (m)	7	17	17	17
RX height (m)	1.5		1.5	
PLE n_{All}	4.5	4.6	1.9	1.8
σ_{All} (dB)	10.8	9.2	1.1	0.1
PLE nBest	3.7	4	—	—
σ_{Best} (dB)	9.5	7.4	—	—
TX gain (dBi)	24.5		24.5	1
TX HPBW (°)	10.9		10.9	28.8
RX gain (dBi)	24.5	15	24.5	15
RX HPBW (°)	10.9	28.8	10.9	28.8
Slope correction factor α	0.71	0.88	0.95	0.9

Table 1. Path loss exponents (PLEs) with respect to a 1 m free space reference distance, and standard deviations obtained for arbitrary pointing angles (n_{All}, σ_{All}) and for the best angles (n_{Best}, σ_{Best}) from the 28 GHz unique pointing angle measurements as a function of environment, TX-RX heights, and TX-RX antenna gains [2]. Measurements were obtained with 15 dBi (28.8° beamwidth) and 24.5 dBi (10.9° beamwidth) TX antennas, and both 24.5 dBi and 15 dBi (10.9° and 28.8° beamwidth) RX antennas.

antennas; thus, true omnidirectional measurements were not originally recorded, but have been developed recently from the directional measurements [13].

Our propagation models are based on modifying the existing microwave FS and SUI path loss models to fit measurement data presented in [2, 4, 8]. The empirical measurement data used in this work is shown in Tables 1 and 2 for both the non-line-of-sight (NLOS) and the clear line-of-sight (LOS) environments for the 28 and 38 GHz mmWave bands, respectively. In these tables, we present the path loss exponent (PLE) and shadow fading statistics with respect to a 1 m free space reference distance for a wide range of locations, where at each location the directional RX antennas were rotated in the azimuth plane at various fixed elevation angles. As described in [2], wherever a link could be made with any pointing angle, the measured power was recorded, and d^n path loss exponent models for arbitrary and best (e.g., angles of strongest received power) pointing angles at the TX and RX were compiled. Thus, these tables may be thought of as providing simple mmWave path loss models that are a function of height and frequency for highly directional, steerable antennas with a specific beamwidth, conditioned on the availability of sufficient signal-to-noise ratio (SNR) for detection at the arbitrary and best pointing angles. The environment definitions used in these tables are now explained.

28 and 38 GHz Measurements and Environment Definitions — RX locations were categorized as either LOS or NLOS according to the following definitions:

- LOS: Both the TX and RX antennas are pointed directly toward each other (i.e., on boresight), and aligned in both the azimuth and elevation planes with no obstructions between the antennas.
- NLOS: Building obstructions exist between the TX and RX. An NLOS environment with moderate obstructions only has trees between the TX and RX, or the RX is just slightly behind a building corner. Also, for directional measurements, NLOS exists for LOS environments, but when the TX and RX antennas are not aligned boresight-to-boresight.

For the 28 GHz propagation campaign, signal was measured and recorded at 28 RX locations in Manhattan, New York City, for three distinct TX locations described in [2] for T-R separation distances up to 200 m. An exhaustive azimuth and elevation sweep was conducted at each RX location using 24.5 dBi (10.9° HPBW) and 15 dBi (28.8° HPBW) gain antennas at both the TX and RX for a maximum system measurement range of 178 dB in order to recover incoming signals from different angles of arrivals. Then PDPs were measured using an 800 MHz null-to-null RF bandwidth sliding correlator channel sounder to determine multipath and path loss data. Measurements were made over distances of 30 to 425 m, but were truncated from 30 to 200 m based on outages.

For the 38 GHz measurements, there were 37 unique receiver locations measured on the campus at the University of Texas at Austin, with six locations measured from two different transmitter locations for a total of 43 unique TX-RX location combinations [4, 8]. Most TX-RX locations used 25 dBi (7.8° HPBW) gain directional antennas at the TX and RX, and the others used 13.3 dBi gain (49.4° HPBW) antennas at the RX. The maximum system measurement range at 38 GHz was 150 dB. The 25 dBi RX antenna measurements covered T-R separation distances between 29 and 930 m, and the 13.3 dBi RX antenna measurements ranged between 29 and 728 m (only 21 unique TX-RX location combinations).

Path Loss Models Using Field Measurements in Urban and Suburban Environments — For both the 28 and 38 GHz measurement campaigns, rotatable high gain horn antennas revealed that buildings, trees, cars, lampposts, and the ground provide a rich scattering environment where multipath signals propagate in many different directions, with vastly different propagation delays (ranging from a few nanoseconds to over 750 ns excess delay in New York City). Unlike the FS and SUI models that assume omnidirectional antennas, the propagation measurements made in [2, 4, 8] used steerable beam antennas and thus have antenna gains associated with the measurements. Tables 1 and 2 present the PLEs and shadow factors w.r.t. a 1 m FS reference distance for single beams obtained with high antenna gains at 28

Frequency: 38 GHz												
Environment	**NLOS**						**LOS**					
TX height (m)	23		8		36		23		8		36	
RX height (m)	1.5											
PLE n_{All}	3.3	2.7	3.8	3.3	3.1	2.7	2.0	2.0	1.9	2.0	1.9	1.9
σ_{All} (dB)	10.6	8.1	11.1	10.7	10.3	8.0	2.3	3.3	8.4	4.3	3.7	1.5
PLE n_{Best}	2.7	2.4	3.2	2.6	2.6	2.4	—	—	—	—	—	—
σ_{Best} (dB)	8.0	6.0	10.3	10.3	8.1	5.1	—	—	—	—	—	—
TX gain (dBi)	25											
TX HPBW (°)	7.8											
RX gain (dBi)	25	13.3	25	13.3	25	13.3	25	13.3	25	13.3	25	13.3
RX HPBW (°)	7.8	49.4	7.8	49.4	7.8	49.4	7.8	49.4	7.8	49.4	7.8	49.4
Slope correction factor α	0.66	0.54	0.62	0.54	0.66	0.58	1.0	1.0	0.95	1.0	0.95	0.95

Table 2. Path loss exponents (PLE) with respect to a 1 m free space reference distance and standard deviations obtained for arbitrary pointing angles (n_{All}, σ_{All}) and the best angles (n_{Best}, σ_{Best}) from the 38 GHz unique pointing angle measurements as a function of environment, TX-RX heights, and TX-RX antenna gains [4]. Measurements were obtained with 25 dBi (7.8° beamwidth) TX antennas, and both 25 dBi and 13.3 dBi (49.4° beamwidth) RX antennas.

and 38 GHz, respectively. The NLOS measurement data in these tables is closely modeled by the environment parameters corresponding to dense and hilly vegetation in the SUI path loss model, while the LOS measurement data may be closely modeled by parameters of the FS path loss model.

In order to modify the omnidirectional SUI path loss model using the 28 and 38 GHz NLOS measurements, we simply find the slope correction factor such that Eq. 1 agrees with the close-in reference free space path loss model [2], which makes use of the PLEs as shown in Tables 1 and 2. Note that the measured results in Tables 1 and 2 were determined by using a 1 m free space reference distance, and were obtained by finding the best minimum mean square error (MMSE) line fit to the 28 and 38 GHz empirical data [2, 4, 8]. The advantage of using the SUI model over the close-in reference free space distance d^n MMSE line fit model given in [2, 4, 8] is that the SUI model has more parameters that allow frequency and height to be adjusted. Thus, the SUI model is more general and well suited to industry for its ease of use and generality. Our Modified SUI model for mmWave in NLOS environments allows us to estimate the path loss in dB, and is of the following form: $PL_{\mathrm{SUI,Mod}}[\mathrm{dB}]\,(d) = \alpha_{\mathrm{NLOS}} \times (PL_{\mathrm{SUI}}(d) - PL_{\mathrm{SUI}}(d_0)) + PL(d_0) + X_{\sigma}$, where α_{NLOS} is the mean slope correction factor (unitless) obtained directly from the NLOS empirical results. The correction factor is obtained by equating the MMSE best-line fit to the SUI relative path loss above the free space reference distance, and solving for the mean slope correction factor. The correction factor obtained this way embodies the difference in slope and intercept between the unmodified SUI model and the close-in free space reference model (MMSE line). Similarly, for a LOS environment, instead of using the SUI model, we use the Friis FS path loss formula, and find the slope correction factor α_{LOS} of the following form: $PL_{\mathrm{FS,Mod}}[\mathrm{dB}](d) = \alpha_{\mathrm{LOS}} \times (PL_{\mathrm{FS}}(d) - PL_{\mathrm{FS}}(d_0)) + PL(d_0) + X_{\sigma}$.

Figure 1 shows the unmodified SUI path loss curve for dense and hilly vegetation (Terrain Type *A*) as shown in Eq. 1, the MMSE best line fit path loss curves obtained for arbitrary pointing angles and best pointing angles (i.e., angles at which strongest power level is received) with the PLEs from Table 1, and the corresponding Modified SUI single beam path loss curve at 28 GHz for the NLOS Manhattan environment with a TX height of 7 m, corresponding to column 1 of Table 1 with a pair of 24.5 dBi directional antennas. From Fig. 1, it is clear that the slope and intercept of the SUI path loss curve are different from those of the MMSE best line fits, which means that the SUI model, as is, cannot be used to estimate realistic observed path loss at mmWave frequencies where directional antennas are used. However, using a slope correction factor of $\alpha = 0.71$ for arbitrary pointing angles from the above analysis, the Modified SUI line shown in Fig. 1 agrees well with the MMSE line fit, and may be used to estimate 28 GHz single beam path loss at arbitrary angles at the TX and RX height of 7 m where 24.5 dB gain antennas are used at both the TX and RX.

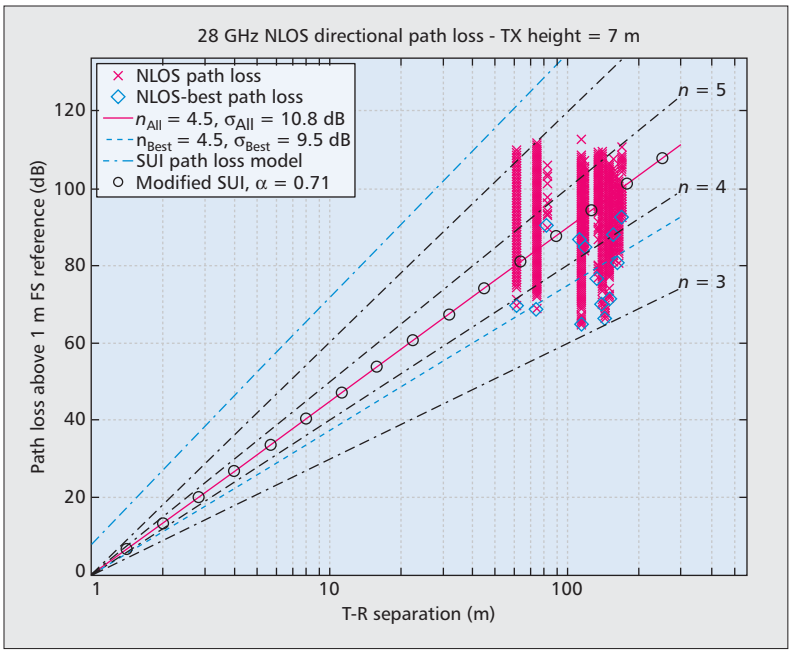

Figure 1. 28 GHz path loss models for a single steerable 10.9° beam at the RX, using today's microwave SUI model, the close-in free space reference distance d^n model from [2], and the Modified SUI model described in this article. The slope correction factor α ensures that the Modified SUI model agrees with the MMSE best line fit to the empirically observed path loss at 28 GHz.

Tables 1 and 2 show the slope correction factors for all 28 and 38 GHz single beam measurements found using the above analysis, and may be used to estimate the path loss for unique pointing angles at the RX for the 28 and 38 GHz frequency bands.

Omnidirectional 28 GHz Path Loss Models — The models presented in the previous section are valid for single narrow beam angular apertures at the receiver, for arbitrary pointing angles where a link may be made, and may be transformed into an omnidirectional path loss model for use with arbitrary antenna patterns at the TX and RX. The 28 GHz measurements collected in Manhattan were further analyzed using three-dimensional ray-tracing techniques in order to recover omnidirectional channel impulse responses with exact propagation timing of each arriving multipath signal that was measured. By synthesizing the exact propagation times of all arriving multipath components from all arriving angles at each measured location, it was possible to synthesize omnidirectional wideband propagation data, as well as total received power for an omnidirectional receiver. Figure 2 shows the d^n omnidirectional close-in reference distance path loss model w.r.t. 1 m in LOS and NLOS environments, derived from the 28 GHz measurements obtained at unique pointing angles [2, 13]. The omnidirectional model was obtained by summing the received power at each unique pointing angle over all azimuth and elevation angles, removing the effects of the 24.5 dBi TX and RX antennas for each individual measured PDP at each angle, and recovering the corresponding path loss at each RX location, thereby simulating the path loss as measured using two 0 dBi isotropic omnidirectional antennas. The PLE was found to be n = 3.4 with a standard deviation of σ = 9.7 dB w.r.t. to a 1 m free space reference distance. The PLE in LOS environments at 28 GHz was found to be n = 2.1, which is relatively close to the expected theoretical free space PLE of n = 2. These values are remarkably similar to today's UHF/microwave systems, with only 8 dB more path loss per decade of distance compared to measured NLOS channels with omnidirectional antennas at 1900 MHz in similar environments [13].

RF Coverage Simulations for Microwave and MmWave Networks

RF Coverage for Microwave Networks Using Existing Path Loss Models

Mobile radio network planners typically try to maintain an average received BS signal strength suitable to the wireless standard of interest. For illustration, let us assume that today's Long Term Evolution (LTE) desired minimum received power $P_{rec}(d)$ of –75 dBm (over the specified future channel bandwidth used) applies to future mmWave systems. From the TX power P_t, the RX signal power at any outdoor location d can be computed as $P_{rec}(d)$[dB] = P_t[dB] – $PL(d)$[dB], where $PL(d)$ is obtained from the path loss model. For $P_{rec}(d)$ to be greater than –75 dBm at any particular location throughout the coverage area, there would need to be sufficient cell density to provide this coverage. For indoor coverage, additional building penetration losses would need to be considered for the external walls and building materials/partitions. For mmWave systems, this will prove especially challenging due to the high penetration losses observed for different building materials [2]. Using the –75 dBm RX signal benchmark and the new mmWave path loss models given here, we used a commercial cellular planning tool, TEMS CellPlanner (TCP) [14], to conduct outdoor RF coverage simulations to compare current microwave and future mmWave networks.

For cellular networks in the UHF/microwave bands, we consider co-located networks where the second-, third-, and fourth-generation (2G, 3G, and 4G) systems are co-located at the same BS sites. Co-location is a cost-effective and popular approach that has helped operators prune down deployment costs for their 3G and 4G networks by sharing sites with 2G systems. In order to maintain the condition $P_{rec}(d) \geq$ –75 dBm for outdoor coverage, we used 43 dBm TX EIRP (for 2G GSM), 43 dBm TX power (for 3G, 4G, and 5G), and the industry standard path loss models from earlier (Hata model, SUI model with terrain type A [10]) to obtain typical cell sizes: $d \leq$ 538 m for 2G, $d \leq$ 372 m for 3G, and $d \leq$ 334 m for 4G. The predicted cell sizes are very similar from a practical point of view; thus, we assume a standard cell radius of 500 m in our analysis for today's existing UHF/microwave net-

works considering the co-location strategy explained above, resulting in site-to-site distances between any two adjacent sites of 1000 m. This agrees with site deployments in typical urban areas, although in major metropolitan areas today, cell site radii may be only 200 m.

We used the following parameters in our simulation [12]: the operating frequencies were set to 0.9 GHz, 2.1 GHz, 2.6 GHz, 28 GHz, and 38 GHz for 2G, 3G, 4G, and 5G path loss estimation, respectively, using the Hata model (for 2G), the SUI model (for 3G and 4G), and the Modified SUI models presented in this work (for 5G). The base and mobile station heights were set to 20 m and 2 m, respectively, with an urban environment type. Finally, the transmit power was set to 43 dBm, with a minimum received power level of –75 dBm.

To explore the impact of mmWave frequencies, we selected a study area of 16 km^2 representing four districts in Riyadh City, Saudi Arabia. Our results are interpreted as percentage of total area (i.e., normalized values) so that they are applicable to urban areas of any size. We used the cellular planning tool in [14] to simulate the RF coverage for each cell, and estimate the total number of cell sites required in the selected area to provide an average outdoor coverage of –75 dBm in co-located 2G/3G/4G sites in the microwave bands.

For an example of a network in today's UHF/microwave bands, we used the planning tool to simulate the RF coverage patterns for 2G GSM sites operating in the 0.9 GHz band. For each of these sites, we used tri-sector cells with directional transmitting antennas at the BS having a 65° HPBW and at heights of 20 m. We also assume a mobile receiver with a receiving antenna height of 2 m. The simulator outputs are presented in Fig. 3a, and may be compared to 5G networks in the mmWave bands. It is observed from this figure that the radiation pattern in the existing 2G networks operating in the microwave bands is extremely amorphous in shape (as illustrated for one BS in this figure). We obtain a realistic cell radius of 518 m in order to maintain outdoor coverage of –75 dBm, which agrees with the calculated data above for the 2G network coverage. The coverage pattern for 3G and 4G systems are similar in shape, as apparent from our coverage calculation results above.

Figure 3a also presents the site locations (red dots) and the network-wide RF coverage simulation results for the co-located 2G/3G/4G cells in the selected area using the simulation parameters quoted above and the path loss models from earlier. From this figure, it can be observed that 22 sites are required to maintain the desired –75 dBm outdoor coverage in the given area. The

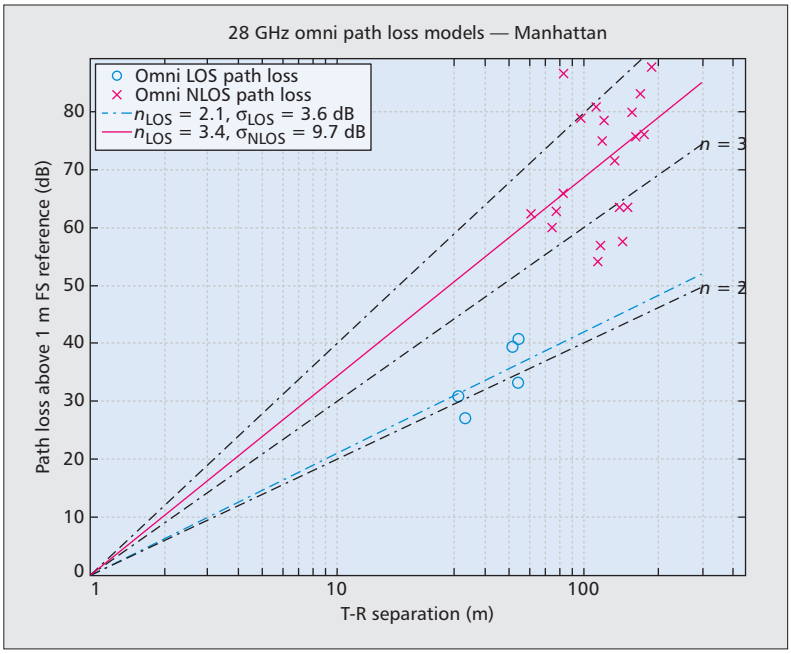

Figure 2. 28 GHz LOS (blue circles) and NLOS (red crosses): omnidirectional close-in reference distance FS path loss models w.r.t. 1 m for two 0 dBi isotropic TX and RX antennas obtained from the 28 GHz measurements [13].

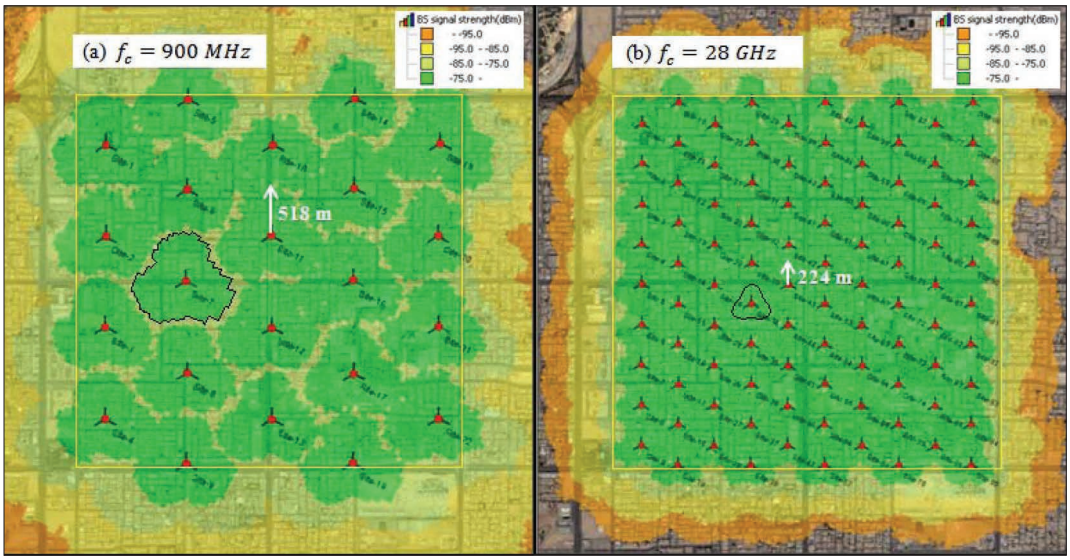

Figure 3. RF coverage prediction for microwave and mmWave based networks: a) microwave networks, f_c = 900 MHz; b) mmWave networks, f_c = 28 GHz.

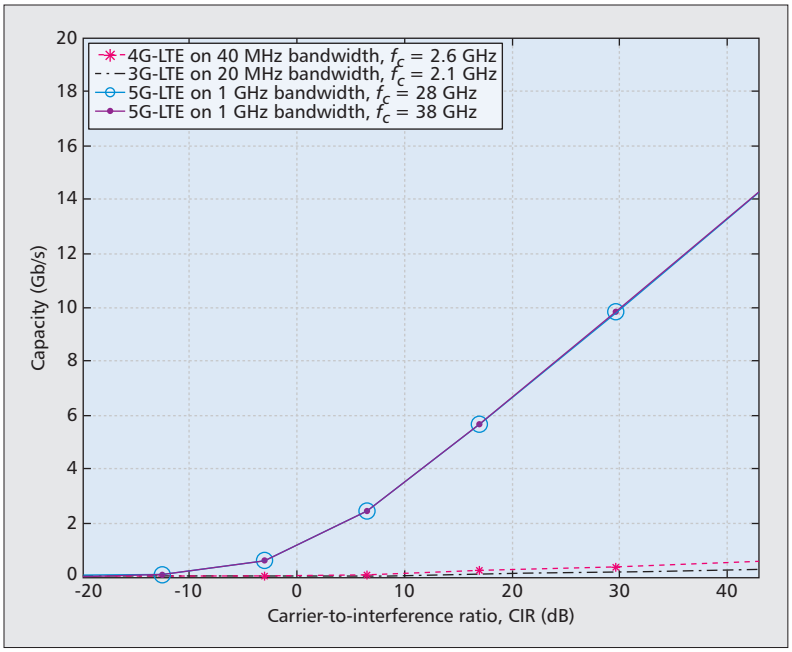

Figure 4. Channel capacity simulation at the current cellular bands at 2.1 GHz and 2.6 GHz for 20 MHz RF bandwidth, and at mmWave bands at 28 and 38 GHz for 1 GHz RF bandwidth.

yellow rectangular box in this figure shows the boundaries of the selected area, and it can be noticed that the outdoor coverage within this boundary is in the desired range of $P_{rec}(d) \geq -75$ dBm, except at the cell edges where the received signal strength is less than –75 dBm. From this result, it is clear that both outdoor and indoor coverage problems may be encountered at some cell-edge areas in the 2G/3G/4G networks, depending on the type of buildings in which the mobile user is located. This result agrees with the current state of the art in the field, where cell edge coverage problems are encountered in 2G/3G/4G networks.

RF Coverage for MmWave 5G Networks Using the Proposed Path Loss Models

This section presents the simulations of RF performance for mmWave cellular systems. Using the proposed mmWave path loss models for arbitrary pointing angles and the coverage prediction simulation tool in [14], we obtain a cell radius of 224 m for an mmWave site to maintain $P_{rec}(d) \geq -75$ dBm outdoor, as illustrated in Fig. 3b. Also using simulation parameters mentioned earlier (with 24.5 dBi antennas at the TX and RX [2]) and the modified path loss SUI models, we obtain the maximum coverage distance d to maintain the condition $P_{rec}(d) \geq -75$ dBm for outdoor coverage of 5G networks in the 28 GHz band as $d \leq 220$ m. These two results agree closely with the 200 m cell radius obtained by field measurements in [2]. For the rest of our simulations in this section, we assume mmWave cell radii of 220 m.

Figure 3b shows the output of the 28 GHz simulation for a cell radius of 220 m with site-to-site distance of 440 m. From Fig. 3b, it is observed that 95 sites are required in a 16 km^2 area to achieve acceptable outdoor coverage in the 28 GHz mmWave band, compared to 22 sites used in the same area for an existing 2G/3G/4G co-located network. In other words, four times the number of existing sites are needed for the mmWave network deployments in the same service area. Since network components are typically more compact for high-frequency devices, deployment costs are not necessarily going to be four times the existing network cost. An exact cost analysis is difficult at this stage since mmWave BSs are not yet available. The data presented above, however, suggests that roughly 330 percent extra BS sites are needed to accommodate 5G networks alongside existing 3G and 4G systems. Therefore, more sites, with lower cost per site, is likely to be the rule for mmWave deployments. Given the difficulty of providing bandwidth to today's cell sites, future mmWave cell sites may use the spectrum for both mobile access as well as backhaul (also called "fronthaul").

The results in Fig. 3b also present a comparison of the network-wide RF coverage for mmWave networks (28 GHz) with their microwave counterpart (900 MHz). From this figure, it is observed that mmWave networks provide better cell- edge coverage than the current microwave-based networks. The occurrence of coverage holes (where $P_{rec}(d) \leq -75$ dBm outdoor) in Fig. 3b is much less compared to those observed in Fig. 3a for the microwave bands, since RF coverage for an mmWave-based site is rounder in shape (as shown for one BS in Fig. 3b) than for RF coverage in the microwave bands shown in Fig. 3a, thanks to the somewhat higher path loss in the mmWave bands, which limits propagation distance away from the BS to similar values in all directions, making tessellation easier. Also in Fig. 3b, the interference caused by an mmWave BS to MSs in the neighboring cells is less than –95 dBm (or insignificant) in all cases for site-to-site distance of 440 m, whereas in Fig. 3a the interference placed by a microwave BS to MSs in the neighboring cells is in the range of –85 dBm to –95 dBm for site-to-site distances of 1000 m, which is considerably more than that experienced in the mmWave system, even though the latter has a shorter site-to-site distance. The end result is improved network-wide outdoor coverage due to less interference in most of the service area for the mmWave system. This indicates that mmWave systems using high gain, steerable beams will be noise limited rather than interference limited — a sharp departure from today's wireless systems. For indoor coverage, however, poor penetrating abilities of mmWave signals [2] implies that cell repeaters or in-building infrastructures may be needed to provide acceptable received power levels inside buildings.

Case of Tracking Best Beam Pointing Angles — If beam tracking technologies are deployed in 5G systems such that BSs form a link with the MSs at any time instant via the single best RF beam pointing directions, lower path loss will be obtained, as shown in Tables 1 and 2, and thus lower TX power will be needed (or range may be extended). Our current commer-

cial simulator cannot model such scenarios. However, using the close-in reference FS distance d^n path loss parameters in Tables 1 and 2 for the best single beam pointing case, we can calculate the achievable coverage for $P_{rec}(d) > -75$ dBm outdoors. If we consider a BS power of 30 dBm (as opposed to 43 dBm for the arbitrary pointing angle case above) and the measurement parameters in the first column of Table 1 (with extra TX and RX antenna gains of 24.5 dBi, PLE $n_{best} = 3.7$), a coverage distance $d = 318$ m can be realized (for 45 percent range extension). Combining two or more beams will provide even greater range [2]. For the case of using the single best antenna beam direction to create a link, this means that only 50 BS sites will be required for the service area under consideration, representing roughly two times the 22 sites used on the same service area (note the extra 13 dB of margin when using arbitrary pointing angle performance) in the co-located 2G/3G/4G systems. In other words, only 127 percent more BSs will be needed in a 5G system operating on this "best pointing beam" tracking principle. However, the probability of obtaining such best links at any time instant must be considered for an accurate RF analysis.

Figure 4 shows a channel capacity simulation comparing 2.1 and 2.6 GHz with 20 MHz RF bandwidth, and the 28 and 38 GHz bands with 1 GHz RF bandwidth. The capacity was estimated in this figure using the expression: $C_{\mathrm{RF}} = \mathrm{BW}\log_2(1 + \mathrm{CIR})$, where BW denotes the RF channel bandwidth of the system, and CIR denotes the carrier-to-interference ratio at various distances from a serving BS. For the tri-sector BS assumed in the simulation setup, there are two interfering cells for a given BS. Therefore, for a site-to-site distance of 1000 m for 2G/3G/4G and 440 m for 5G, we estimated CIR as

$$\mathrm{CIR}_{\mathrm{dB}} = 10\log_{10}\left(\frac{P_{rec}(d)}{2P_{rec}(D-d)}\right),$$

where D denotes the site-to-site distance and d is the desired distance from the BS where the CIR is to be estimated. It can be seen from Fig. 4 that the capacity for 5G systems is over 20 times that of today's 4G systems, which agrees with the findings in [3], demonstrating the usefulness of the proposed path loss models in estimating 5G link performance.

Conclusion

This article presents new path loss models suitable for cellular planning in the 28 and 38 GHz mmWave bands that stem from simple modifications of current path loss models used in commercial planning tools. The proposed models accurately estimate mmWave path loss data that match observations in both heavy and light urban areas. Using the new mmWave propagation models, we simulate the RF coverage for future 5G cellular networks. An effective cell radius of about 220 m is simulated, which agrees closely with recent measurements conducted at 28 GHz [2]. Based on the simulation results, it is observed that with completely random beamforming, 5G networks would require roughly three times the number of sites deployed currently in the same coverage area, but when considering the single best beams, only two times more sites will be needed compared to the existing 2G/3G/4G co-located networks. For multibeam combining, cell coverage will increase further, requiring even fewer additional sites compared to today's networks. Capacity for the random pointing case yields over 20 times the capacity of today's cell networks using available mmWave spectrum, and we expect an additional increase in capacity when using the single best pointing beams and multibeam combining.

Capacity for the random pointing case yields over 20 times the capacity of today's cell networks using available mmWave spectrum, and we expect an additional increase in capacity when using the single best pointing beams and multibeam combining.

Acknowledgment

This work was supported by NSTIP strategic technologies programs at King Saud University (11-ELE1854-02) in the Kingdom of Saudi Arabia.

References

[1] Z. Pi and F. Khan, "An Introduction to Millimeter-Wave Mobile Broadband Systems," *IEEE Commun. Mag.*, vol. 49, no. 6, June 2011, pp. 101–07.

[2] T. S. Rappaport *et al.*, "Millimeter Wave Mobile Communications for 5G Cellular: It Will Work!," *IEEE Access*, vol. 1, May 2013, pp. 335–49.

[3] S. Rangan, T. S. Rappaport, and E. Erkip, "Millimeter-Wave Cellular Wireless Networks: Potentials and Challenges," *Proc. IEEE*, vol. 102, no. 3, Mar. 2014, pp. 366–86.

[4] T. S. Rappaport *et al.*, "Broadband Millimeter-Wave Propagation Measurements and Models Using Adaptive-Beam Antennas for Outdoor Urban Cellular Communications," *IEEE Trans. Antennas and Propagation*, vol. 61, no. 4, Apr. 2013, pp. 1850–59.

[5] F. Khan, Z. Pi, and S. Rajagopal, "Millimeter-Wave Mobile Broadband with Large Scale Spatial Processing for 5G Mobile Communication," *Proc. IEEE 50th Annual Allerton Conf.*, Oct. 2012, pp. 1517–23.

[6] T. S. Rappaport, J. N. Murdock, and F. Gutierrez, "State of the Art in 60 GHz Integrated Circuits and Systems for Wireless Communications," *Proc. IEEE*, vol. 99, no. 8, Aug. 2011, pp. 1390–436.

[7] S. Akoum, O. El Ayach, and R. W. Heath, "Coverage and Capacity in mmWave Cellular Systems," *Proc. IEEE Conf. 46th Asilomar Conf.*, Nov. 2012, pp. 688–92.

[8] J. N. Murdock *et al.*, "A 38 GHz Cellular Outage Study for an Urban Campus Environment," *Proc. IEEE Wireless Commun. Net. Conf.*, Apr. 2012, pp. 3085–90.

[9] Masaharu Hata, "Empirical Formula for Propagation Loss in Land Mobile Radio Services," *IEEE Trans. Vehic. Tech.*, vol. VT-29, no. 3, Aug. 1980, pp. 317–25.

[10] P. D. Katev, "Propagation Models for Wimax at 3.5 GHz," *IEEE-Elektro 2012 Conf.*, 2012, pp. 61–65.

[11] T. S. Rappaport, *Wireless Communications: Principles and Practice*, 2nd ed., Prentice-Hall, 2002.

[12] A. T. Nassar, A. I. Sulyman, and A. Alsanie, "Achievable RF Coverage and System Capacity Using Millimeter Wave Cellular Technologies in 5G Networks," *Proc. IEEE-CCECE 2014*, Toronto, Canada, May 2014.

[13] G. R. MacCartney, M. K. Samimi, and T. S. Rappaport, "Omnidirectional Path Loss Models in New York City at 28 GHz and 73 GHz," *IEEE Personal, Indoor, and Mobile Radio Communications*, Sept. 2–5, 2014.

[14] TEMS CellPlanner (TCP) tool: http://www.mentum.com, accessed Aug. 2013.

Biographies

Ahmed Iyanda Sulyman [SM'09] (asulyman@ksu.edu.sa) obtained his Ph.D. degree from the Department of Electrical and Computer Engineering, Queen's University, Canada, in 2006. He was a teaching fellow at Queen's University in 2004–2006, and a postdoctoral fellow at the Royal Military College of Canada in 2007–2009. He joined the Department of Electrical Engineering at King Saud University, Saudi Arabia, in 2009, where he is currently an associate professor. He has published over 50 journal/conference articles in the area of wireless communications.

ALMUTHANNA T. NASSAR is a radio access network planning specialist manager in the Mobile Radio Network Planning and Design Department, Etihad Etisalat Company (mobily), Riyadh, Saudi Arabia. He has more than seven years of practical experience in radio frequency planning and optimization. He received his B.S. degree in electrical engineering from Jordan University of Science and Technology, Irbid, Jordan, in 2006. He is currently working toward his M.S. degree in electrical engineering at King Saud University.

MATHEW K. SAMIMI received his B.S. degree in applied physics from the Fu Foundation School of Engineering and Applied Sciences of Columbia University, New York, in 2012, and his M.S. degree in electrical engineering from the New York University (NYU) Polytechnic School of Engineering, Brooklyn, New York, in 2014, where he is currently pursuing his Ph.D. degree in electrical engineering with Prof. Rappaport in developing future millimeter-wave statistical spatial channel models for next generation ultra-wideband mobile cellular in dense urban environments.

GEORGE R. MACCARTNEY JR. received B.S. and M.S. degrees in electrical engineering from Villanova University, Pennsylvania, in 2010 and 2011, respectively. He is currently working toward his Ph.D. degree in electrical engineering at the NYU Polytechnic School of Engineering with Prof. T. S. Rappaport, focused on millimeter-wave propagation and modeling for 5G communication systems. Since January 2013, he has been with NYU WIRELESS, NYU Polytechnic School of Engineering.

THEODORE S. RAPPAPORT (tsr@nyu.edu) received his Ph.D. degree from Purdue University in 1987. He has founded three major academic wireless research centers as a faculty member at Virginia Tech from 1988–2002, the University of Texas at Austin from 2002–2012, and most recently at NYU, where he is the David Lee/Ernst Weber Chair of Electrical and Computer Engineering, and founding director of NYU WIRELESS. He has advised over 100 students and has co-authored several best-selling wireless textbooks. His latest book, *Millimeter Wave Wireless Communications*, has just been published by Pearson/Prentice-Hall.

ABDULHAMEED ALSANIE (sanie@ksu.edu.sa) received his Ph.D. degree from the Department of Electrical and Computer Engineering, Syracuse University, New York, in 1992. He has been with the Department of Electrical Engineering at King Saud University (KSU), Saudi Arabia, since 1983, where he is currently working as an associate professor and department chair.